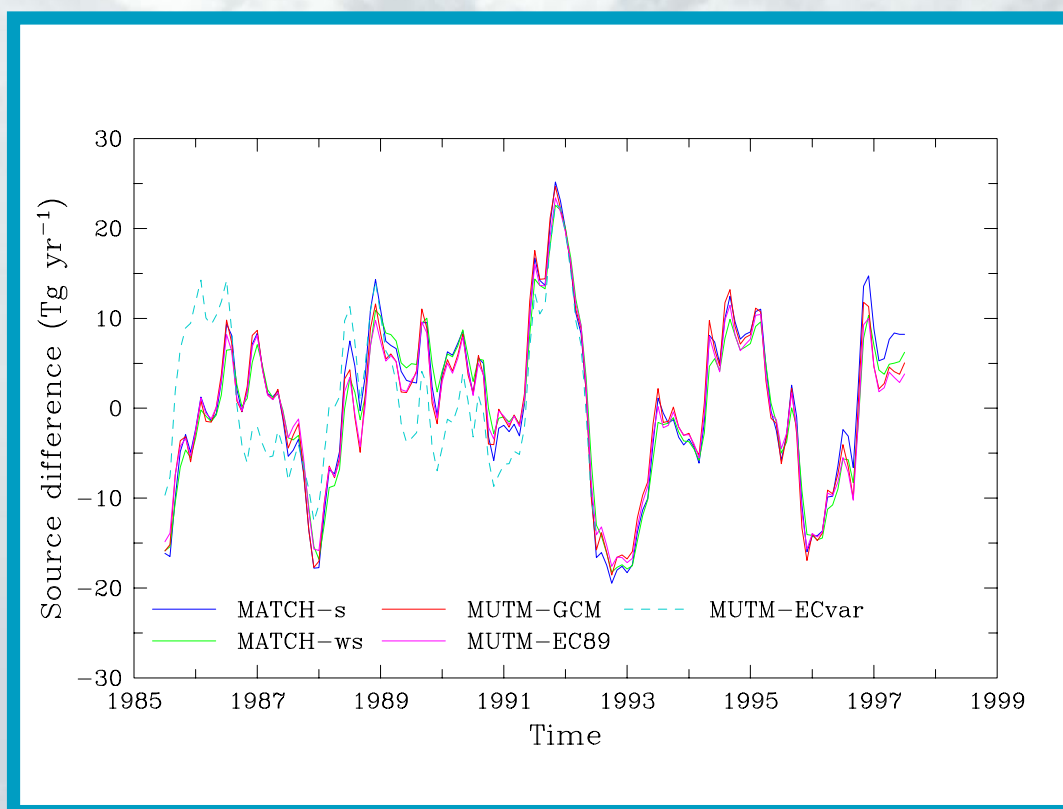


Methane sources from mass-balance inversions: Sensitivity to transport

R.M. Law and P.F. Vohralik



Atmospheric Research

Methane sources from mass-balance inversions: Sensitivity to transport

R.M. Law
CSIRO Atmospheric Research

P.F. Vohralik
CSIRO Telecommunications and Industrial Physics

National Library of Australia Cataloguing-in-Publication Entry

Law, Rachel Mary

Methane sources from mass-balance inversions: Sensitivity to transport

Bibliography.

ISBN 0 643 06644 6

1. Atmospheric methane - Measurement. 2. Atmospheric methane - Observations. 3. Sinks (Atmospheric chemistry).

I. Vohralík, Peter Frederic. II. CSIRO. Division of Atmospheric Research. III. Title. (Series: CSIRO Atmospheric Research technical paper; no. 50).

551.5112

Address and contact details: CSIRO Atmospheric Research
Private Bag No.1 Aspendale Victoria 3195 Australia
Ph: (+61 3) 9239 4400; fax: (+61 3) 9239 4444
e-mail: chief@dar.csiro.au

CSIRO Atmospheric Research Technical Papers may be issued out of sequence.

Methane sources from mass-balance inversions: Sensitivity to transport

R.M. Law

CSIRO Atmospheric Research, Private Bag 1,
Aspendale, Vic 3195, Australia

P.F. Vohralik

CSIRO Telecommunications and Industrial Physics,
PO Box 218, Lindfield, NSW 2070, Australia

Abstract

Two different three-dimensional tracer transport models are run with various subgrid-scale parameterizations and dynamics data to estimate zonal mean methane sources from observed concentrations of methane. The observations used are the monthly mean methane data for thirteen years from the NOAA/CMDL network. The atmospheric sink of methane through chemical loss is modelled using loss rates from the CSIRO two-dimensional chemical transport model. The zonal mean structure and seasonal cycles of the estimated methane sources show some sensitivity to the transport model used. Interannual variability of the sources is less sensitive to transport but is sensitive to the choice of observational data used to constrain the inversion. This limits the interpretation of the variability obtained although the impact of the Mt Pinatubo eruption does appear to be evident in the calculated sources.

1 Introduction

Methane is a greenhouse gas whose atmospheric concentration has increased significantly since pre-industrial times. This increase has been tracked through ice-core, firn, air-archive and flask data (Etheridge et al., 1998). Methane growth rates have varied considerably over the last 50 years, peaking in the early 1980s. The recent slow-down in methane growth (e.g. Steele et al., 1992) has been used to imply a stabilization in methane sources (Dlugokencky et al., 1998). Global methane sources can be estimated from the increase in atmospheric concentration of methane provided the lifetime of methane is known. The lifetime is determined by destruction of methane (CH_4) in the troposphere by reaction with hydroxyl radicals (OH) and to a smaller extent by reaction with OH, chlorine (Cl) and $\text{O}(^1\text{D})$ in the stratosphere.

The role of methane as a greenhouse gas and the need to predict its future atmospheric concentration means that it is important to understand how recent methane sources have evolved. Clearly anthropogenic CH_4 fluxes have increased significantly over the industrial period but there are also large natural fluxes of CH_4 that are influenced by climatic variations. CH_4 sources can be estimated through two main methods: scaling up local, process-based measurements (e.g. Sass et al. (1999) for rice cultivation) or using atmospheric methane measurements to infer sources, a so-called inverse method. These inverse methods require a two- or three-dimensional transport model to calculate atmospheric concentrations from surface emissions.

Several groups have performed methane inversions using a variety of methods. Fung et al. (1991) used a three-dimensional (3-D) model to perform a synthesis inversion. For each methane source, they assumed the geographical distribution was known and adjusted the source strength. They found a preferred methane budget but also found that the methane observations were not able to distinguish between a number of different possible budgets. Brown (1995) used a two-dimensional (2-D) model and a singular value decomposition-based method for her inversion. She produced quite different results to Fung et al. and attributed this to the initialisation procedure used. Hein et al. (1997) extended the work of Fung et al. to a Bayesian methodology. This uses the prior source estimates and uncertainties as input to the inversion and produces error estimates on the resulting source uncertainties. They found uncertainty reductions of up to 40% for some source components. These inversions estimated mean methane sources. Saeki et al. (1998) used a mass-balance inversion method with a 2-D model to estimate the time evolution of sources from 1983 to 1994. They found little overall trend in global emissions but increasing emissions for 0°-30°N and decreasing emissions for 30°-90°N. Houweling et al. (1999) extended the work of Hein et al., again using a Bayesian inversion approach. However they were able to estimate methane sources at grid-point resolution by using the adjoint of their transport model. They found a reduction in source strengths in SE Asia compared to the prior estimates. They also noted that their uncertainty reductions were generally smaller than those found by Hein et al.

In any inversion method, the modelled transport is assumed to be perfect. There are, as yet, no inversion methods that are able to account for transport model error explicitly, although those methods that account for data uncertainties can include a contribution due to estimates of the ability of the model to simulate data at a particular location. Both Hein et al. (1997) and Saeki et al. (1998) have tested the sensitivity of their inversions to changes in transport within their models. Hein et al. compared an inversion run using 1986 winds with another using 1987 winds. They found differences in source estimates were small compared to the uncertainties on those estimates. Saeki et al. increased and decreased the transport coefficients in their 2-D model. They found that changes in meridional diffusion changed the distribution of sources between hemispheres by up to 10 Tg yr⁻¹, while changes in vertical diffusion changed the global source by 2 Tg yr⁻¹ but had little impact on the latitudinal distribution. These sensitivity tests examined the impact of changes in transport within a given transport model. In this work, we examine transport sensitivity further by performing the same methane inversion with different transport models, different subgrid-scale transport parameterizations and different wind fields. The models and method are outlined in the following section. We assess the impact on both the mean methane sources calculated and the interannual variability of the sources. The sensitivity obtained is contrasted to that due to changing the observational data with which the inversion are forced.

2 Method

Methane sources can be estimated from atmospheric concentrations. This requires a transport model with some representation of the chemical loss of methane and an inversion method. There are two main types of inversion, typically called ‘synthesis’ and ‘mass-balance’, each

with advantages and disadvantages. The main difference between the methods is how they deal with the limited data available to force the inversion. The mass-balance method interpolates the data to give greater spatial data coverage while synthesis methods estimate only regional sources or source components. The main advantage of synthesis inversions is the ability to include uncertainty analysis while an advantage of mass-balance inversions is the ability to include interannually-varying transport. In either case, the inversion is dependent on the transport model, which is assumed to be perfect. Transport model intercomparisons for forward calculations of species such as CO₂ (Law et al., 1996), SF₆ (Denning et al., 1999) and radon (Jacob et al., 1997) all show significant variations between different transport models. Here we use a simple inversion to illustrate the impact of transport model and wind field variations on the methane source calculation.

2.1 Inversion method

We chose to use a mass-balance inversion similar to that used for CO₂ by Law and Simmonds (1996). In this method, the tracer model surface concentrations are constrained to ‘observed’ values. The model is run forward in time and the difference between the modelled and observed values defines the required surface source or sink. The difficulty with this method is the need to define surface concentrations at all latitudes and longitudes in order to estimate a two-dimensional source field. For most trace gases there are insufficient measurements to define longitudinal variations, particularly during the early years of the measurement record. Consequently we assume that longitudinal variations are negligible and fit the data only in the north-south direction (described below). The inversion is then constrained with a zonally-uniform distribution. While sources are estimated at all model gridpoints, only zonal mean sources will be analysed since any longitudinal variations represent transport effects only.

2.2 Data

Atmospheric methane concentrations are measured at approximately 60 sites around the globe and on some aircraft flights and ship cruises. Most of these sites are part of the NOAA/CMDL network. Measurements began in 1983 at 17 sites; by 1997 measurements were available at about 40 sites and from Pacific Ocean and South China Sea cruises (Dlugokencky et al., 1994). Since one aspect of the results that we will consider is interannual variability, it may be important to keep an approximately constant network during the period being considered. Hence, most of the experiments described here use monthly mean data from 20 sites from 1985-1997 (NOAA/CMDL ftp site, August 1998 release). The 20 sites are chosen as those whose records spanned 1985-1997 even if there were gaps in the record (not more than 12 missing months were allowed at the start or end of the period). The network used is shown in Figure 1. A brief comparison is also made with inversions using smaller and larger networks. These networks are also shown in Figure 1. We have not used sites such as Mauna Loa where the air is not expected to be representative of the lowest model level.

The data are assumed to be representative of the latitude of the site and a spline has been fitted to describe the meridional distribution of CH₄ concentration. The spline was fitted in sine latitude with a 50% attenuation at 0.707 (45°). The mean (1985-1997) fit for each month is shown in Figure 2. The concentration gradient is large through the tropics with high concentrations in the north and lower concentrations in the south. Concentrations are lower in summer than winter in both hemispheres.

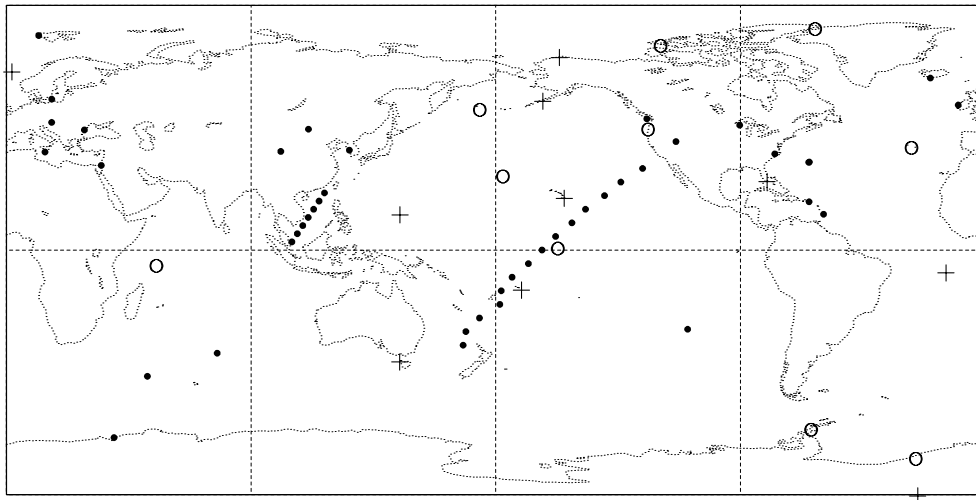


Figure 1: CH₄ observation sites used to constrain the inversion. The control case is the 20 sites indicated by the plus signs and open circles. The plus signs indicate the 10-site subset of the control case. The solid circles indicate the extra sites used in the all-sites case.

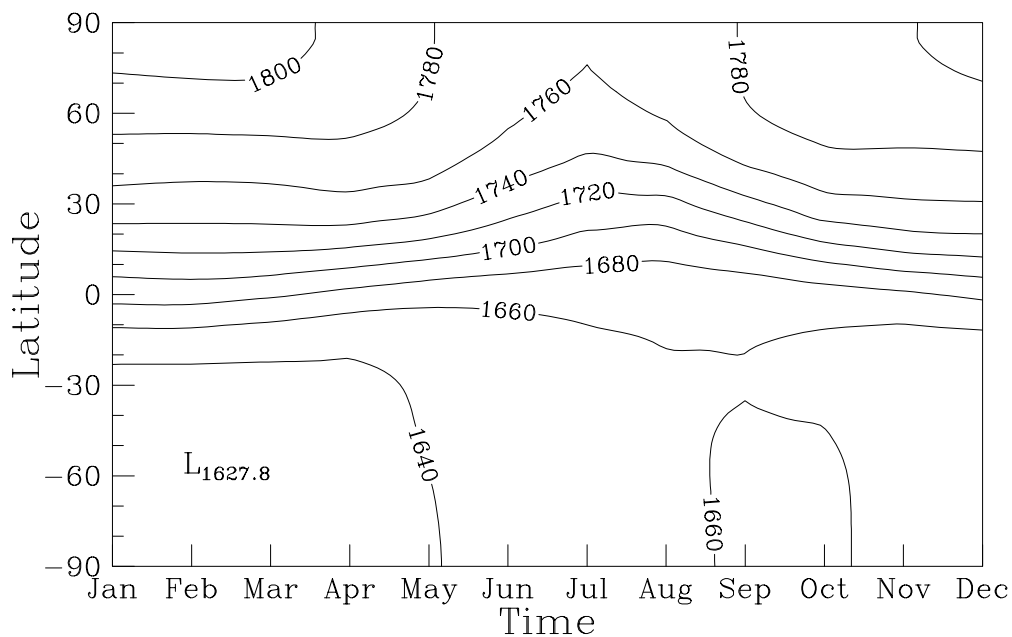


Figure 2: Mean 1985-1997 methane concentration in ppb calculated from the spline fits to the monthly observations.

2.3 Chemical loss

The mass-balance inversion determines only surface sources and sinks but there is also a large chemical sink for methane. Most methane is destroyed by reaction with OH in the troposphere and approximately 10% by reactions with OH, Cl and O(¹D) in the stratosphere. These loss processes must be accounted for within the transport model.

It is not currently possible to measure OH on a global scale and therefore climatologies of OH and methane loss derived from measurements are not generally available. However, these quantities can be estimated using chemical transport models (e.g. Spivakovsky et al., 1990). The OH fields obtained from chemical transport models can be assessed and rescaled if needed by simulating methyl chloroform, which has relatively well-known sources and is removed primarily by reaction with OH in the troposphere (e.g. Hein et al., 1997).

There is some debate over whether OH concentrations have changed over recent decades. Prinn et al. (1995) found no significant change in OH between 1978 and 1994 based on observations of methyl chloroform while Krol et al. (1998) find a small positive trend in OH using the same data but a different modelling approach. Karlsdóttir and Isaksen (2000) find a similar positive trend in OH in a 3-D model study for 1980-1996 where the model was forced by observed CH₄ concentrations and estimates of anthropogenic emissions of CO, NO_x and NMHCs. In addition to any long term trend, it is expected that there is interannual variability in OH concentrations. For example, Dlugokencky et al. (1996) estimated a decrease in OH of 7-8% after the eruption of Mount Pinatubo due to decreased UV actinic flux from increased SO₂ and sulfate aerosols.

The change in methane due to chemical loss at a given location in the atmosphere is calculated using

$$\Delta q = -Lq\Delta t \quad (1)$$

where q is methane mixing ratio (concentration), Δt is the time step and L is the effective first-order rate coefficient for methane loss at that location. For the present study, methane loss rates were obtained from the CSIRO 2-D chemical transport model (CTM). The CSIRO 2-D CTM used for the present study has been described by Vohralik et al. (1998) and is also discussed in Park et al. (1999), Kawa (1999), WMO (1998) and Penner et al. (1999). Given that the primary focus of the present study is on the sensitivity of the inversion calculations to changes in model transport, using methane loss rates from a 2-D CTM rather than from a 3-D CTM is not expected to affect the conclusions reached.

Total methane loss rates L from the CSIRO 2-D CTM were archived at 10-day intervals on the 2-D model pressure-latitude grid for one year. Thus seasonal variations are included but not interannual variations. These loss rates were then linearly interpolated to the 3-D transport model levels using global annual mean surface pressure, and linearly interpolated in latitude and time as required. The loss rates L used for the 3-D inversion studies were assumed to be independent of longitude.

Loss rates were obtained from a calculation using the CSIRO 2-D CTM constrained as follows. Mixing ratios of N₂O, CH₄, CH₃Cl, CCl₄, CH₃Br, the halons, the chlorofluorocarbons (CFCs)

and the hydrochlorofluorocarbons (HCFCs) were fixed at the lowest model level to values projected for the year 2015, as given in Table 4.2A of Kawa (1999). Ground-level O₃ is held fixed at 20 ppbv. Sulphate aerosol surface areas used correspond to the enhanced (median) level of aerosols given in Table 8-8 of WMO (1992), which represents the median values over the two decades prior to 1992. Rate coefficients were taken from DeMore et al. (1997). In addition, the CO mixing ratio at the lowest model level was fixed at 100 ppbv at all latitudes, and NO_x surface sources were held constant at 6×10^9 (N atoms) cm⁻²s⁻¹ at all latitudes. Reactions on polar stratospheric clouds, non-methane hydrocarbons, and aircraft emissions were not included in the calculations.

Initial tests with these loss rates indicated a total methane loss (using one transport model) of approximately 400 Tg yr⁻¹. Given that the CSIRO 2-D model has been used primarily for stratospheric studies, and does not include a detailed representation of tropospheric processes, it was decided to increase the loss rates by a factor of 1.125 in order to give a total methane loss of about 450 Tg yr⁻¹ from the initial 3-D runs. This value is used by Fung et al., (1991) in their preferred methane budget scenario.

It is clear that the loss rates used here limit the conclusions that can be drawn from the inversions that we will perform. The lack of longitudinal and interannual variation in loss rate, the calculation of the loss rates under 2015 rather than 1990 conditions and the somewhat arbitrary rescaling of the loss rates means that the source estimates that we obtain should not be considered best estimates. However, provided broadly plausible sources are obtained, the conclusions about sensitivity to transport and data network should be robust. For these sensitivity tests, the important constraint is that the loss rates used are the same across all inversions rather than that the detailed spatial and temporal structure of those loss rates are correct.

2.4 Transport models

Two transport models have been used. The first is a variant of the National Center for Atmospheric Research Model of Atmospheric Transport and Chemistry (NCAR-MATCH) (Rasch et al., 1997). Here we run the model with six-hourly, annually-repeating Middle Atmosphere Community Climate Model version 2 (MACCM2) dynamics data, which have been reduced to 24 levels by removing 20 levels in the stratosphere. The model runs on hybrid levels, which are constant pressure levels above about 70 hPa and mixed pressure sigma levels below. The top model level is at 0.025 hPa. This is the same configuration as used in Law and Rayner (1999) for CO₂. Removing levels does have some impact on cross-tropopause transport, the implications of which will be discussed later. The model's horizontal resolution is 5.625° in longitude and 2.8° in latitude and advective transport uses a semi-lagrangian scheme.

The subgrid-scale transport by vertical diffusion and convection is parameterised. Two versions of the model are used with different vertical diffusion schemes. The first takes precalculated diffusivities from the MACCM2 simulation, which were calculated using a non-local boundary-layer based scheme (Holtslag and Boville, 1993). The scheme determines the planetary boundary layer (PBL) height and calculates diffusivities based on stability, separately for the PBL and

free troposphere. The second scheme is the turbulent vertical transport parameterization from the Melbourne University general circulation model (GCM) (Simmonds, 1985). The scheme is a mixing length scheme but based only on the wind shear, not thermodynamic stability. Diffusive transport is determined from the temperature and wind forcing fields and the modelled tracer concentrations. Maximum mixing lengths are greater in the lower half of the atmosphere. The first scheme has much greater differentiation of vertical mixing over land and ocean than the second. We refer to the first scheme as the stability dependent scheme and the second as the wind-shear dependent scheme. More details are given in Law and Rayner (1999) where the two model versions are shown to produce quite different seasonal covariance behaviour for CO₂. There are two convection schemes in the NCAR-MATCH model that are usually run in parallel (see Appendix of Rasch et al. (1997)). However the MACCM2 dynamics data only contain the necessary fields to run one of the schemes. Therefore, in this model, subgrid mixing due to vertical diffusion tends to dominate over mixing due to convective transport.

The second transport model (MUTM) is derived from the Melbourne University GCM (Simmonds, 1985). The transport model has a rhomboidal 21 wave spectral resolution in the horizontal (equivalent to 64×54 grid points) and 9 vertical sigma levels. Subgrid-scale processes of horizontal and vertical diffusion and convective transport are included. The vertical diffusion scheme used here is the same as the wind-shear dependent version used in MATCH while the convection scheme is based on statistics of convection occurrences in the parent GCM. The model is described more fully by Law et al. (1992) and is compared with other tracer transport models simulating CO₂ in Law et al. (1996). This comparison showed that this model tends to produce more rapid tracer mixing than other models when used with wind fields from the Melbourne University GCM. The wind fields are input daily (there is no diurnal cycle) and one year of winds is usually used repeatedly when multi-year simulations are required. The model is also run with European Centre for Medium-range Weather Forecasting (ECMWF) analysed winds as described by Dargaville et al. (2000) for CO₂. The winds have been interpolated to the model grid and from pressure levels to the model sigma levels. The 12-hourly data have been averaged to give daily values. The ECMWF data are used to drive both the advection and the vertical diffusion parameterization but convective transport remains dependent on the GCM statistics. Only 1985-1992 data were available to us. We run the model both with one year of winds (we chose 1989) repeatedly and with the full eight years of data.

2.5 Experiments

A set of experiments has been run to calculate sources from 1985-1997. The initial conditions are taken from a previous methane simulation and rescaled to match the surface mean concentration at the start of this experiment. The model is then run for a further two years using the 1985 concentration surface fields extrapolated back in time based on the methane growth rate during 1985. After this initialisation, sources are then calculated for 13 years using the 1985-1997 20-site data fits to constrain the model. Five cases are run using the five model configurations available; MATCH with stability-dependent vertical diffusion (MATCH-s), MATCH with wind-shear dependent vertical diffusion (MATCH-ws), MUTM with MUGCM winds (MUTM-GCM), MUTM with ECMWF 1989 winds (MUTM-EC89) and MUTM with

ECMWF 1985-1992 winds (MUTM-ECvar).

It is important to note that, while all the experiments are forced with interannually varying concentration data, only one (MUTM-ECvar) includes interannually varying transport and none include interannual variations in the chemical loss of methane. The results that we obtain for interannual variability in methane source will need to be interpreted in the context of this limitation in the experiment.

A second set of experiments uses one model (MATCH-s) but surface concentration constraints derived from 10 sites or all surface sites to compare with the 20-site case. This will give some indication of how the sensitivity to data network size compares to the sensitivity to transport model.

3 Results and discussion

We examine three aspects of the calculated sources; the 1985-1997 mean latitudinal distribution, the 1985-1997 mean seasonal cycle and the interannual variability. The seasonal cycles and interannual variability are analysed for 6 regions: global, high latitudes (50° - 90° S and N), mid-latitudes (15° - 50° S and N) and the tropics (15° S- 15° N).

3.1 Latitudinal distribution

Zonal-mean 1985-1997 CH_4 sources are shown in Figure 3. (The MUTM-ECvar case is the 1985-1992 mean). Each model configuration gives maximum sources around 35° - 40° N with a secondary maximum close to the equator. Sources are substantially larger in the northern hemisphere than the southern hemisphere as would be expected. Sources integrated globally and regionally are given in Table 1. While the general distribution of sources is similar for the different model cases there are also several differences that warrant explanation.

The global surface source is approximately 50 Tg yr^{-1} smaller using MATCH than using MUTM. Most of this difference is due to the behaviour of the two models in their upper layers. MATCH, as noted earlier, appears to have slower cross-tropopause transport using the reduced (24-level) wind set compared to the full 44-level MACCM2 data. This results in very low CH_4 concentrations in the upper model layers and consequently low chemical loss of CH_4 in the stratosphere. Since the global surface source is controlled by the growth of atmospheric methane and the total chemical loss, the surface source is consequently smaller. MUTM by contrast has low vertical resolution and a poorly defined stratosphere, which results in relatively high CH_4 concentrations in the top two model levels, especially for the cases run with ECMWF winds. This results in a larger loss and consequently a larger surface source. We should note that neither result is correct given our knowledge of typical stratospheric CH_4 concentrations but highlights one of the difficulties of running these inversions with models with low vertical resolution in the stratosphere. Overall the total source is smaller than most recent estimates

(note that the source here includes any surface soil sink) but the global source is highly dependent on the total chemical loss of methane, which we know may not be well characterized by the simplified loss rates used here.

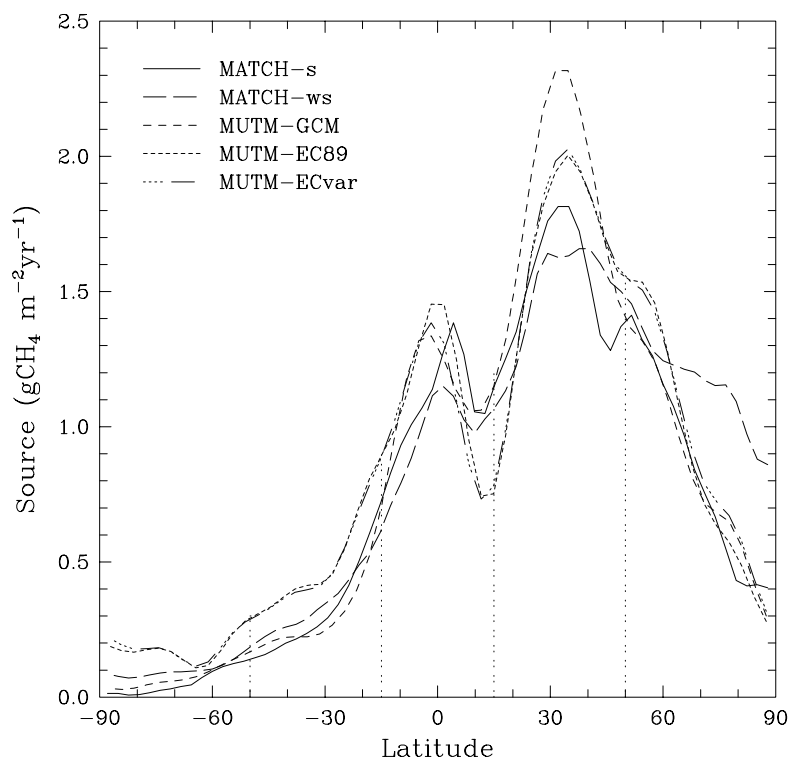


Figure 3: Zonal mean 1985-1997 methane source in $\text{gCH}_4 \text{ m}^{-2} \text{ yr}^{-1}$. The line identification is given in the key. The MUTM-ECvar case is the mean of 1985-1992. The vertical lines indicate the regions that sources are integrated over in Table 1.

Model	Global	50°-90°N	15°-50°N	15°S-15°N	15°-50°S	50°-90°S
MATCH-s	448.9	61.1	196.1	144.0	43.2	4.5
MATCH-ws	447.2	74.5	191.2	128.2	46.6	6.7
MUTM-GCM	495.2	60.6	239.1	150.0	39.9	5.6
MUTM-EC89	499.2	67.0	208.1	147.9	65.5	10.7
MUTM-ECvar	496.8	68.3	210.4	142.7	64.5	11.0

Table 1: Regional CH_4 Sources in Tg yr^{-1} for 1985-1997. The MUTM-ECvar case is for 1985-1992.

In the high northern latitudes, the MATCH-ws case produces larger fluxes than the other models (6-14 Tg yr^{-1} larger over the 50°-90° region). This larger source is indicative of more mixing of CH_4 out of this region in the MATCH-ws case. It is likely that this is a result of the vertical

diffusion scheme used in this case, which has less seasonal dependence than the scheme used in the MATCH-s case and consequently allows some mixing all year round and more mixing overall. While the MUTM cases also use this diffusion scheme, they produce a smaller vertical CH_4 gradient in the lower troposphere (presumably due to more vigorous advective mixing) so mixing by vertical diffusion has a smaller net impact.

The MUTM-EC results show little sensitivity to being run with one year of winds repeatedly or with varying winds. The EC cases produce smaller northern hemisphere sources and larger southern hemisphere sources than MUTM run with GCM winds. This is because the GCM winds produce greater interhemispheric transport than the ECMWF winds and consequently require a larger interhemispheric difference in source to maintain the observed north-south CH_4 gradient.

3.2 Seasonal cycles

Mean seasonal cycles of the estimated sources are shown in Figure 4 for the globe and in Figure 5 for each region. The seasonal cycles are represented by the difference in flux for the mean of that month from the annual mean flux for 1985-1992. This allows for a more direct comparison of the magnitude of the seasonality between model cases. The global results indicate maximum sources in the northern summer with a peak in September. The largest difference between model cases is in June and July when the MATCH simulations give larger sources than the MUTM simulations.

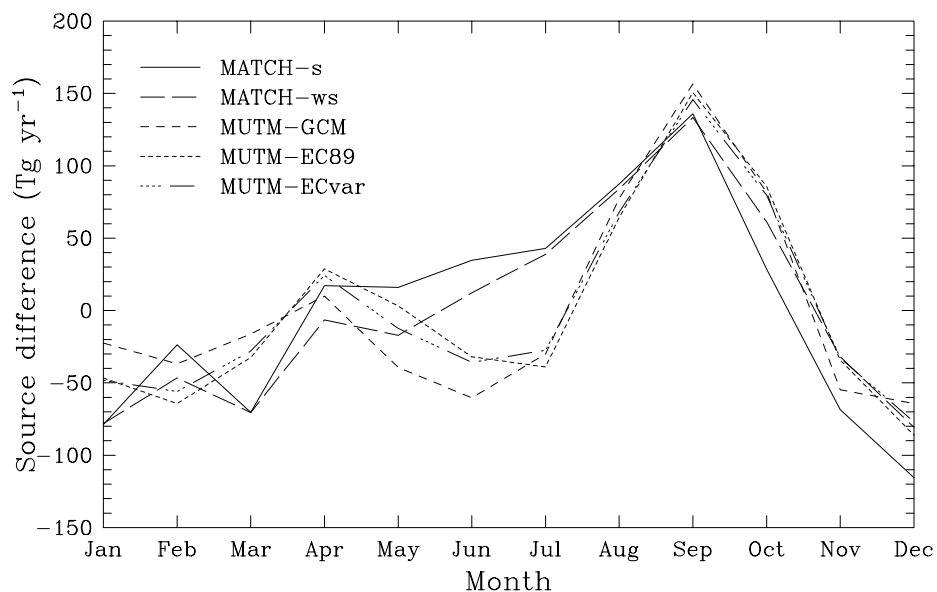


Figure 4: Mean seasonal cycle of global CH_4 source. The monthly fluxes are in Tg yr^{-1} and the mean 1985-1992 source appropriate to each case has been subtracted. The line identification is given in the key.

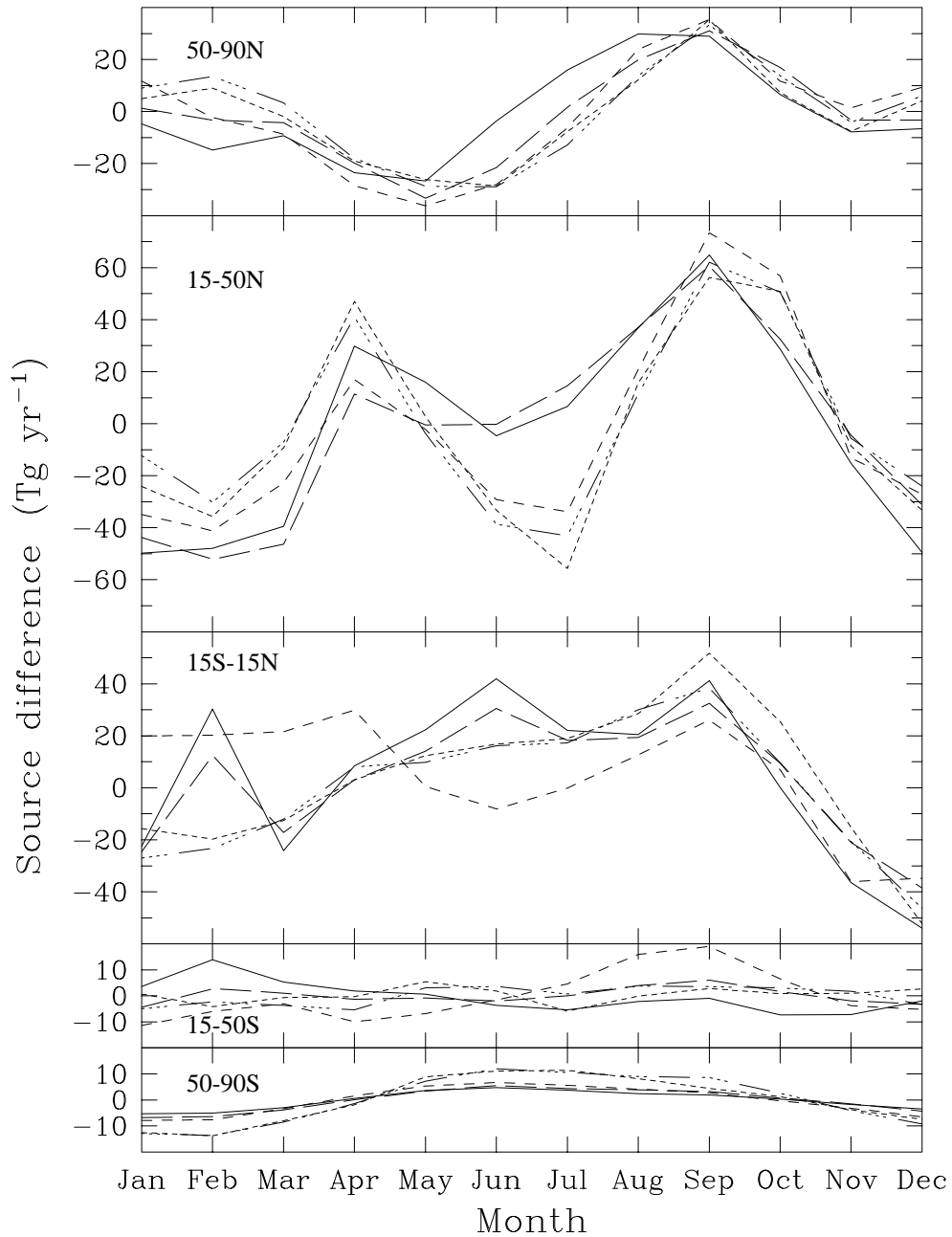


Figure 5: Mean seasonal cycle of regional CH_4 sources for MATCH-s (solid), MATCH-ws (long dash), MUTM-GCM (short dash), MUTM-EC89 (dotted) and MUTM-ECvar (dash-dot). The region is given at the left side of each panel. The monthly fluxes are in Tg yr^{-1} and the mean 1985-1992 source appropriate to each case and region has been subtracted.

The regional seasonal cycles show that the global result is dominated by the seasonality in the 15°-50°N region. This shows two maxima in April and September separated by a minimum in June-July. The minimum is much more pronounced in the MUTM cases than in the MATCH cases. Seasonal cycles are smaller in the northern high-latitudes and tropics. In the northern region, the maximum source is in September, with the exception of the MATCH-s case in which the summer increase in source occurs earlier by about a month. This is because the vertical diffusion scheme used in the MATCH-s case produces more diffusive transport over land in summer in this region than the diffusion scheme used in all the other cases. The extra vertical mixing in the MATCH-s case must be compensated for by an increased source in order to maintain the observed CH₄ concentrations.

The tropics generally show a mid-year maximum although in this case the MUTM-GCM case is somewhat different, matching the September maximum that the other cases produce but showing a different seasonality to the other cases during the first half of the year. The large methane gradient across the tropics means that the sources are likely to be quite sensitive to the horizontal winds in this region and the model's positioning of the intertropical convergence zone (ITCZ). For example, the February maximum in the MATCH cases appears to be consistent with an equatorial zonal-mean *v*-component wind that is less negative in February than January or March in the MACCM2 winds. This would mean less transport of high concentration air from the north and a consequent need for a greater source in February to maintain the surface concentrations.

Seasonality in the southern regions is small, as would be expected. In general it is understood that the observed seasonality in southern hemisphere concentrations is driven largely by the seasonality in chemical loss of methane due to the seasonality in OH concentration (Prather et al., 1995). Loss is larger in summer and smaller in winter. The calculated sources for 50°-90°S show a minimum in summer and maximum in winter. This could imply that the seasonality of loss rates used here is too small. A sensitivity test was run using MUTM in which the seasonality of methane loss was doubled but the mean loss was unchanged. This gave smaller (close to zero) seasonality in southern middle to high latitude sources and an increased seasonality in tropical sources. In the northern mid-latitudes, winter sources were decreased and summer sources increased such that the June-July minimum became less pronounced. There was little impact on the northern high-latitude source seasonality.

3.3 Interannual variability

Interannual variability as represented by the 12-month running mean source (as a difference from the 1985-1992 mean source) is shown in Figure 6 for global sources and Figure 7 for regional sources. The global source ranges over 30-40 Tg yr⁻¹ with the smallest source around late 1992 and the largest source around late 1991. There is no real trend in the source over the 1985-1997 period in agreement with the result of Dlugokencky et al. (1998). However we should recall that our study assumes constant methane loss rates and that of Dlugokencky et al. assumes a constant methane lifetime, an assumption that has recently been challenged (Krol et al., 1998; Karlsdóttir and Isaksen, 2000). The interannual variability in the sources shows

almost no sensitivity to the model configuration used, with the exception of the case run with ECMWF varying winds.

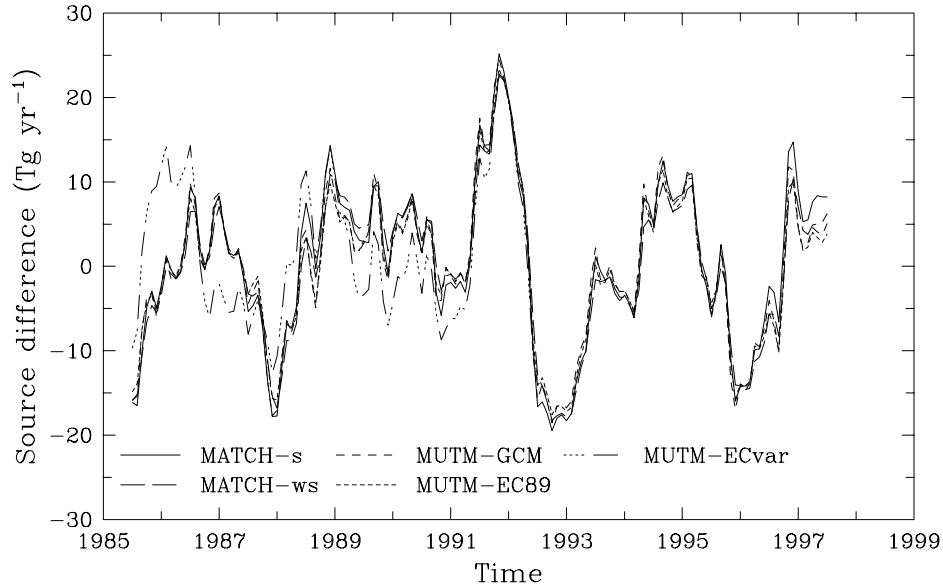


Figure 6: 12-month running mean global CH_4 source in Tg yr^{-1} . The mean 1985-1992 source appropriate to each case has been subtracted. The line identification is given in the key.

The difference with the varying wind case results from the relatively low vertical resolution of MUTM and its consequent poor representation of the stratosphere. Stratospheric loss of methane results in a significant gradient in methane between the top two levels of the transport model. This gradient is also dependent on the transport of methane into the top model layer. There is sufficient variation in this transport in the different years of ECMWF data (at least when interpolated onto the transport model grid) that top level concentrations can vary by over 100 ppb. When the inversion is run with consecutive years of winds, the top level model concentrations are dominated by these transport-related variations, swamping any forcing from the surface concentration constraint. Since the surface source is ultimately dependent on changes in CH_4 concentration averaged over the whole atmosphere, the large concentration variations in the top model layer are sufficient to ‘corrupt’ the source estimates. It would seem then, that the interannual variability of the sources cannot be reliably estimated using this particular combination of interannually varying winds and low resolution transport model. Whether this result applies more generally is an important question for future work.

As occurs at the global scale, the interannual variability of regional sources (Figure 7) is very similar between transport cases. (The EC-var case is not shown because of the uncertainty in these sources at the global scale.) Interannual variability is largest in the tropics. There is an apparent decrease in sources in the northern regions and an increase in sources in the tropics across the 1985-1997 time period. The different cases produce variability that is very similar in phasing although the magnitudes of the maxima and minima do vary more at the regional scale compared to the global scale. In general the MUTM-GCM run gives larger variability than the

other cases. This is consistent with this model producing greater interhemispheric transport than the other cases since greater transport requires a larger source anomaly to maintain any imposed concentration anomaly.

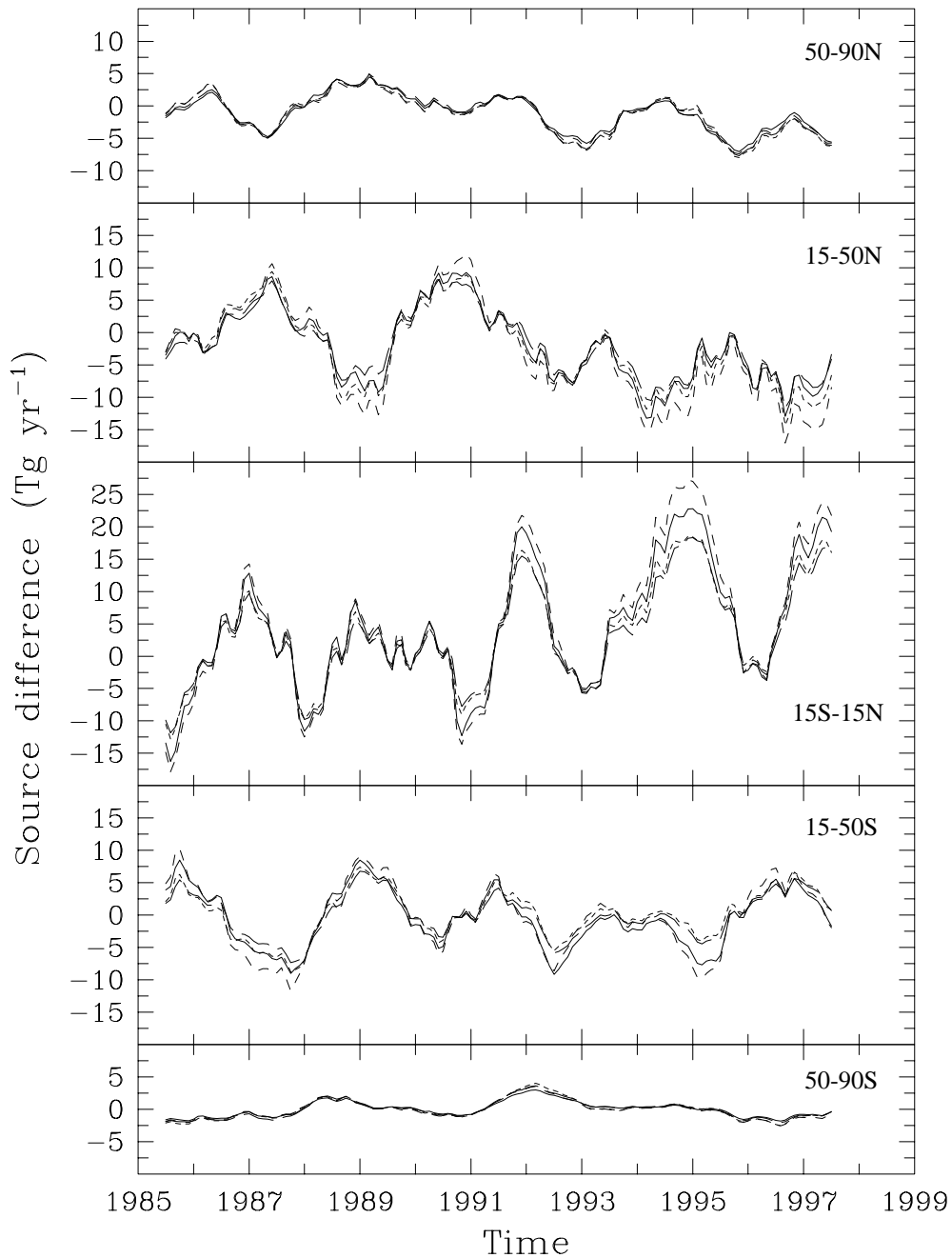


Figure 7: 12-month running mean regional CH₄ sources in Tg yr⁻¹ for MATCH-s (solid), MATCH-ws (long dash), MUTM-GCM (short dash) and MUTM-EC89 (dotted). The region is given at the right side of each panel. The mean 1985-1992 source appropriate to each case and region has been subtracted.

The sensitivity of interannual variability to the transport model can be compared to the sensitivity to the data network used to provide the inversion forcing. Global interannual variability is shown in Figure 8. The 20-site case is the same as the MATCH-s case in Figure 6. There is greater sensitivity to the data network than there was to the transport model. However there is still an overall consistency in the interannual variability, which suggests that on a global scale, interannual variations are adequately captured even with a small network.

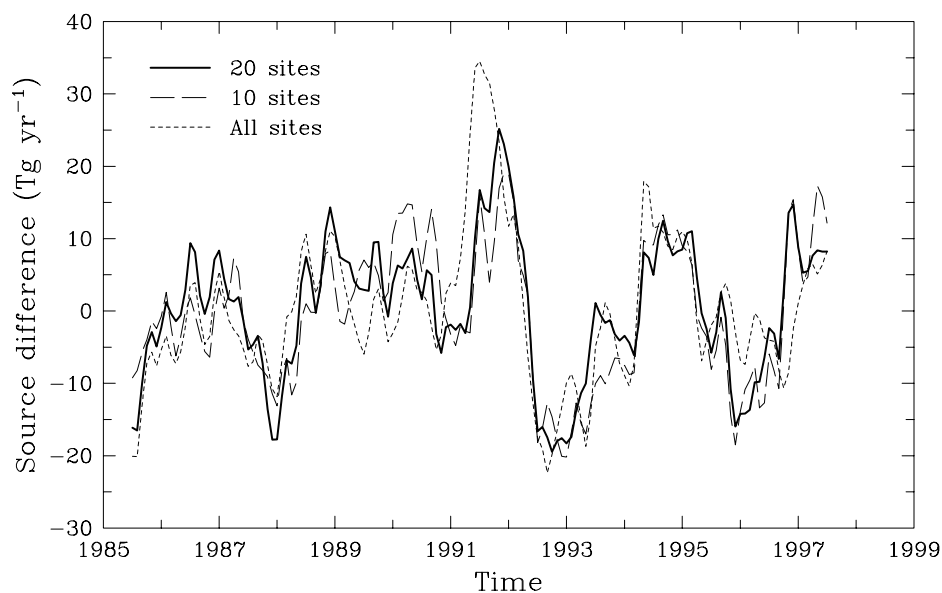


Figure 8: 12-month running mean global CH_4 source in Tg yr^{-1} for various data networks. The mean 1985-1992 source appropriate to each case has been subtracted. The line identification is given in the key.

The largest inconsistency is in the magnitude and timing of the late 1991 maximum. This maximum is related to the Mt Pinatubo eruption. The associated decrease in OH results in decreased methane loss. Since the methane loss rates in the inversion include no variability, the inversion deduces an increased source of methane. It would seem likely that the larger magnitude in the large network case is due to the inclusion of sites that are closer to Mt Pinatubo (e.g. South China Sea, $3^\circ\text{-}20^\circ\text{N}$, $105^\circ\text{-}117^\circ\text{E}$; Quinghai, 36.3°N , 100.9°E and Tae-Ahn, 36.7°N , 126.1°E). However the records for these sites begin only during 1991, which makes it difficult to distinguish between the impact on the inversion of introducing data at new locations as opposed to the impact of volcano-influenced data.

The minimum, in late 1992 and early 1993, found in all cases is also likely to be related to the Pinatubo eruption. A decrease in stratospheric ozone should result in greater tropospheric UV and therefore an increase in OH. The resulting perturbation in methane is interpreted by the inversion as a decreased source because climatological loss rates are used.

The interannual variability of regional sources is shown in Figure 9. This shows much larger differences between the sets of sources than both the network global-scale results and the transport regional-scale results. For all regions, the 10-site case shows greater variability than the

20-site case. This suggests that the north-south fit is not well constrained by only 10 sites and the inversion is consequently quite vulnerable to any unrepresentative data. The apparent trends seen in the 20-site case for the tropics and northern regions are not seen when only 10 sites are used.

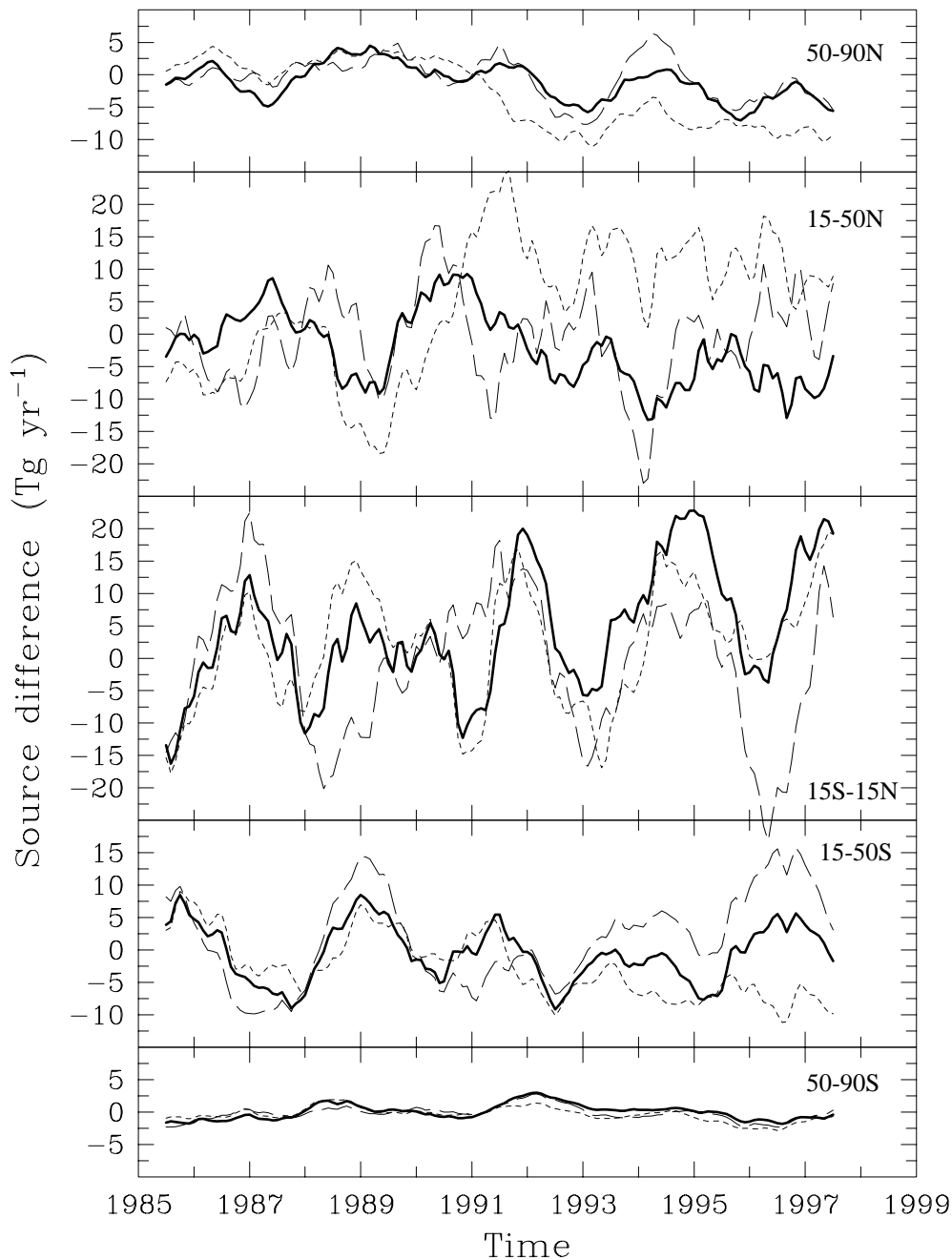


Figure 9: 12-month running mean regional CH₄ sources in Tg yr⁻¹ for the 20-site case (solid, bold), the 10-site case (long dash) and the all site case (short dash). The region is given at the right side of each panel. The mean 1985-1992 source appropriate to each case and region has been subtracted.

The ‘all-sites’ case is often reasonably similar to the 20-site case in the early period of the inversion. This is because the all-site case has few additional sites through the early years. In the southern mid-latitude region, the all-sites case gives smaller sources from about 1994 onwards. This appears to be due to the inclusion of the Easter Island record (30°S) beginning in 1994. From about 1992, the northern regions show a shift in source from the high latitudes to the mid-latitudes in the all-site case compared to the 20-site case. This occurs because of an increasing number of sites with closer proximity to methane sources in the northern midlatitudes. These tend to measure higher concentrations than the sites at high latitude and so the mid-latitude source is increased. Clearly the all-site case could not be reliably used for identifying trends in regional sources. It is interesting to note that the extra global source in the all-site case in 1991 occurs in the northern mid-latitude region. The tropical region sources are relatively unchanged around this time.

4 Summary and conclusions

It is useful to summarize the relative sensitivities to transport and network using a simple measure; the root mean square (rms) difference between each case and the MATCH-s case. We consider first the interannual variability using the 12-month running mean time series of sources (Figures 6-9). For global sources, the transport cases produce rms differences of 1.6-1.9 Tg yr⁻¹ while for the network cases, the rms differences are 4.7 and 6.9 Tg yr⁻¹. Similar relative magnitudes are seen at the regional scale, with the rms differences between network cases always larger (from about 2 to 6 times larger) than the rms differences for the transport cases.

By contrast, the sensitivity of the 1985-1997 zonal mean source to data network (not shown) is smaller than the sensitivity due to transport (shown in Figure 3). Again this can be confirmed in the rms differences (calculated with appropriate area-weighting) from the MATCH-s sources. Rms differences for the transport cases range from 0.18-0.21 gCH₄ m⁻² yr⁻¹ while in the network cases, the rms differences are 0.04 and 0.10 gCH₄ m⁻² yr⁻¹ for the 10- and all-site cases respectively. As one might anticipate, on the seasonal timescale the relative sensitivity of sources to network or transport is more mixed. In the transport cases, the rms differences (both global and regional) between the MATCH-s and MATCH-ws are smaller than between MATCH-s and any of the MUTM cases, suggesting that the choice of transport model is important. The rms differences from the network cases are generally smaller than, or comparable with, the MATCH-s/MATCH-ws differences. An exception is the difference for the 10-site case in the tropics, which is larger than the tropical differences for any other case (transport or network). In the 10-site case the tropical sources are largely forced by the data from Ascension Is (8°S), which samples mostly southern hemisphere air. In the 20-site case, Seychelles and Christmas Island are also used with more northern hemisphere influence. There is a consequent change to the seasonality of the tropical sources.

These results imply that decisions about how an inversion is run should depend on what information is sought from the inversion. If long-term mean sources are required then choices of data network may be less important than ensuring the transport is well modelled. If the interannual variability of sources is required then more care should be taken in making data choices than in

making transport choices. The work done on data extension techniques, described by Masarie et al., (1995) for CO₂ and now applied to CH₄ (GLOBALVIEW-CH₄, 1999), may be useful for reducing this network sensitivity.

While the various simplifications to the inversion (e.g. zonally-uniform loss rates and forcing concentrations) preclude any detailed assessment of these emissions, the inversion does produce plausible methane emissions. Further work to improve these estimates would need to include longitudinal variations in both surface forcing and methane loss rates. Interannual source variability would benefit from interannually varying methane loss and the impact of interannually varying winds should also be tested using a transport model with higher vertical resolution. Ultimately, the inversion should be performed with a model that includes fully interactive chemistry.

Acknowledgments

This study was carried out with support from the Australian Government Cooperative Research Centres Programme. We acknowledge, with thanks, the use of National Oceanic and Atmospheric Administration (NOAA), Climate Monitoring and Diagnostics Laboratory (CMDL), Carbon Cycle Group methane observations. We thank Drs Ian Plumb and Peter Rayner for helpful comments on the text.

References

- Brown, M., The singular value decomposition method applied to the deduction of the emissions and the isotopic composition of atmospheric methane, *J. Geophys. Res.*, *100*, 11,425–11,446, 1995.
- Dargaville, R. J., R. M. Law, and F. Pribac, Implications of interannual variability in atmospheric circulation on modelled CO₂ concentrations and source estimates, *Global Biogeochem. Cycles*, *14*, 931–943, 2000.
- DeMore, W. B., S. P. Sander, D. M. Golden, R. F. Hampson, M. J. Kurylo, C. J. Howard, A. R. Ravishankara, C. E. Colb, and M. J. Molina, Chemical kinetics and photochemical data for use in stratospheric modeling, *Technical Paper 97-4*, JPL, 1997.
- Denning, A. S., et al., Three-dimensional transport and concentration of SF₆: A model inter-comparison study (TransCom 2), *Tellus*, *51B*, 266–297, 1999.
- Dlugokencky, E. J., P. M. Lang, K. A. Masarie, and L. P. Steele, Atmospheric CH₄ records from sites in the NOAA/CMDL air sampling network, in *Trends '93: A Compendium of Data on Global Change*, edited by T. Boden, D. Kaiser, R. Sepanski, and F. Stoss, 274–350, Carbon Dioxide Information Analysis Center, Oak Ridge, U.S.A, 1994.

Dlugokencky, E. J., E. G. Dutton, P. C. Novelli, P. P. Tans, K. A. Masarie, K. O. Lantz, and S. Madronich, Changes in CH₄ and CO growth rates after the eruption of Mt. Pinatubo and their link with changes in tropical tropospheric UV flux, *Geophys. Res. Lett.*, *23*, 2761–2764, 1996.

Dlugokencky, E. J., K. A. Masarie, P. M. Lang, and P. P. Tans, Continuing decline in the growth rate of the atmospheric methane burden, *Nature*, *393*, 447–450, 1998.

Etheridge, D. M., L. P. Steele, R. J. Francey, and R. L. Langenfelds, Atmospheric methane between 1000 AD and present: evidence for anthropogenic emissions and climate variability, *J. Geophys. Res.*, *103D*, 15,979–15,993, 1998.

Fung, I., J. John, J. Lerner, E. Matthews, M. Prather, L. P. Steele, and P. J. Fraser, Three-dimensional model synthesis of the global methane cycle, *J. Geophys. Res.*, *96*, 13,033–13,065, 1991.

GLOBALVIEW-CH₄, Cooperative Atmospheric Data Integration Project - Methane, CD-ROM, NOAA/CMDL, Boulder, Colorado, 1999, [Also available on Internet via anonymous FTP to ftp.cmdl.noaa.gov, Path: ccg/ch4/GLOBALVIEW].

Hein, R., P. J. Crutzen, and M. Heimann, An inverse modeling approach to investigate the global atmospheric methane cycle, *Global Biogeochem. Cycles*, *11*, 43–76, 1997.

Holtslag, A. A. M., and B. A. Boville, Local versus nonlocal boundary-layer diffusion in a global climate model, *J. Climate*, *6*, 1825–1842, 1993.

Houweling, S., T. Kaminski, F. Dentener, J. Lelieveld, and M. Heimann, Inverse modeling of methane sources and sinks using the adjoint of a global transport model, *J. Geophys. Res.*, *104*, 26,137–26,160, 1999.

Jacob, D. J., et al., Evaluation and intercomparison of global atmospheric transport models using ²²²Rn and other short-lived tracers, *J. Geophys. Res.*, *102*, 5953–5970, 1997.

Karlsdóttir, S., and I. S. A. Isaksen, Changing methane lifetime: Possible cause for reduced growth, *Geophys. Res. Lett.*, *27*, 93–96, 2000.

Kawa, S. R., Assessment of the effects of high-speed aircraft in the stratosphere, *Technical Paper 209237*, NASA, Hampton, Va, 150pp, 1999.

Krol, M., P. J. van Leeuwen, and J. Lelieveld, Global OH trend inferred from methylchloroform measurements, *J. Geophys. Res.*, *103*, 10,697–10,711, 1998.

Law, R., and I. Simmonds, The sensitivity of deduced CO₂ sources and sinks to variations in transport and imposed surface concentrations, *Tellus*, *48B*, 613–625, 1996.

Law, R., I. Simmonds, and W. F. Budd, Application of an atmospheric tracer model to the high

southern latitudes, *Tellus*, 44B, 358–370, 1992.

Law, R. M., and P. J. Rayner, Impacts of seasonal covariance on CO₂ inversions, *Global Biogeochem. Cycles*, 13, 845–856, 1999.

Law, R. M., et al., Variations in modelled atmospheric transport of carbon dioxide and the consequences for CO₂ inversions, *Global Biogeochem. Cycles*, 10, 783–796, 1996.

Masarie, K. A., and P. P. Tans, Extension and integration of atmospheric carbon dioxide data into a globally consistent measurement record, *J. Geophys. Res.*, 100, 11,593–11,610, 1995.

Park, J. H., M. K. Ko, C. H. Jackman, R. A. Plumb, J. Kaye, and K. H. Sage, Models and measurements intercomparison II, *Technical Memorandum 209554*, NASA, Hampton, Va, 502pp, 1999.

Penner, J. E., D. H. Lister, D. J. Griggs, D. J. Dokken, and M. McFarland, Aviation and the global atmosphere, a special report of IPCC working groups I and III., *Technical report*, IPCC, Cambridge UK, 1999.

Prather, M., R. Derwent, D. Ehhalt, P. Fraser, E. Sanhueza, and X. Zhou, Other trace gases and atmospheric chemistry, in *Climate Change 1994: Radiative Forcing of Climate Change and An Evaluation of the IPCC IS92 Emission Scenarios*, edited by J. Houghton, L. M. Filho, J. Bruce, H. Lee, B. Callander, E. Haites, N. Harris, and K. Maskell, 73–126, Cambridge University Press, 1995.

Prinn, R. G., R. F. Weiss, B. R. Miller, J. Huang, F. N. Alyea, D. M. Cunnold, P. J. Fraser, D. E. Hartley, and P. G. Simmonds, Atmospheric trends and lifetime of CH₃CCl₃ and global OH concentrations, *Science*, 269, 187–192, 1995.

Rasch, P., N. M. Mahowald, and B. E. Eaton, Representations of transport, convection and the hydrologic cycle in chemical transport models: Implications for the modeling of short lived and soluble species, *J. Geophys. Res.*, 102, 28,127–28,138, 1997.

Saeki, T., T. Nakazawa, M. Tanaka, and K. Higuchi, Methane emissions deduced from a two-dimensional atmospheric transport model and surface measurements, *J. Meteor. Soc. Japan*, 76, 307–324, 1998.

Sass, R. L., F. M. Fisher Jr., A. Ding, and Y. Huang, Exchange of methane from rice fields: National, regional, and global budgets, *J. Geophys. Res.*, 104, 26,943–26,951, 1999.

Simmonds, I., Analysis of the ‘spinup’ of a general circulation model, *J. Geophys. Res.*, 90, 5637–5660, 1985.

Spivakovsky, C. M., S. C. Wofsy, and M. J. Prather, A numerical method for parameterization of atmospheric chemistry: Computation of tropospheric OH, *J. Geophys. Res.*, 95, 18,433–18,439, 1990.

Steele, L. P., E. J. Dlugokencky, P. M. Lang, P. P. Tans, R. C. Martin, and K. A. Masarie, Slowing down on the global accumulation of atmospheric methane during the 1980's, *Nature*, 358, 313–316, 1992.

Vohralik, P. F., L. K. Randeniya, I. C. Plumb, and K. R. Ryan, Use of correlations between long-lived atmospheric species in assessment studies, *J. Geophys. Res.*, 103, 3611–3627, 1998.

World Meteorological Organization (WMO), Scientific assessment of ozone depletion: 1991, *WMO Rep. 25*, WMO, Geneva, 1992.

World Meteorological Organization (WMO), Scientific assessment of ozone depletion: 1998, *WMO Rep. 44*, WMO, Geneva, 1998.

CSIRO Atmospheric Research Technical Papers

This series has been issued as *Division of Atmospheric Research Technical Paper* (nos. 1–19); *CSIRO Division of Atmospheric Research Technical Paper* (nos. 20–37) and *CSIRO Atmospheric Research Technical Paper* from no. 38.

Regular electronic publication commenced with no. 45. Earlier technical papers are progressively being made available in electronic form. A current list of technical papers is maintained at <http://www.dar.csiro.au/info/TP.htm>. Papers may be issued out of sequence.

- No. 1 Galbally, I.E.; Roy, C.R.; O'Brien, R.S.; Ridley, B.A.; Hastie, D.R.; Evans, W.J.F.; McElroy, C.T.; Kerr, J.B.; Hyson, P.; Knight, W.; Laby, J.E. *Measurements of trace composition of the Austral stratosphere: chemical and meteorological data*. 1983. 31 p.
- No. 2 Enting, I.G. *Error analysis for parameter estimates from constrained inversion*. 1983. 18 p.
- No. 3 Enting, I.G.; Pearman, G.I. *Refinements to a one-dimensional carbon cycle model*. 1983. 35 p.
- No. 4 Francey, R.J.; Barbetti, M.; Bird, T.; Beardsmore, D.; Coupland, W.; Dolezal, J.E.; Farquhar, G.D.; Flynn, R.G.; Fraser, P.J.; Gifford, R.M.; Goodman, H.S.; Kunda, B.; McPhail, S.; Nanson, G.; Pearman, G.I.; Richards, N.G.; Sharkey, T.D.; Temple, R.B.; Weir, B. *Isotopes in tree rings*. 1984. 86 p.
- No. 5 Enting, I.G. *Techniques for determining surface sources from surface observations of atmospheric constituents*. 1984. 30 p.
- No. 6 Beardsmore, D.J.; Pearman, G.I.; O'Brien, R.C. *The CSIRO (Australia) Atmospheric Carbon Dioxide Monitoring Program: surface data*. 1984. 115 p.
- No. 7 Scott, John C. *High speed magnetic tape interface for a microcomputer*. 1984. 17 p.
- No. 8 Galbally, I.E.; Roy, C.R.; Elsworth, C.M.; Rabich, H.A.H. *The measurement of nitrogen oxide (NO, NO₂) exchange over plant/soil surfaces*. 1985. 23 p.
- No. 9 Enting, I.G. *A strategy for calibrating atmospheric transport models*. 1985. 25 p.
- No. 10 O'Brien, D.M. *TOVPIX: software for extraction and calibration of TOVS data from the high resolution picture transmission from TIROS-N satellites*. 1985. 41 p.
- No. 11 Enting, I.G.; Mansbridge, J.V. *Description of a two-dimensional atmospheric transport model*. 1986. 22 p.
- No. 12 Everett, J.R.; O'Brien, D.M.; Davis, T.J. *A report on experiments to measure average fibre diameters by optical fourier analysis*. 1986. 22 p.
- No. 13 Enting, I.G. *A signal processing approach to analysing background atmospheric constituent data*. 1986. 21 p.
- No. 14 Enting, I.G.; Mansbridge, J.V. *Preliminary studies with a two-dimensional model using transport fields derived from a GCM*. 1987. 47 p.
- No. 15 O'Brien, D.M.; Mitchell, R.M. *Technical assessment of the joint CSIRO/Bureau of Meteorology proposal for a geostationary imager/sounder over the Australian region*. 1987. 53 p.
- No. 16 Galbally, I.E.; Manins, P.C.; Ripari, L.; Bateup, R. *A numerical model of the late (ascending) stage of a nuclear fireball*. 1987. 89 p.

- No. 17 Durre, A.M.; Beer, T. *Wind information prediction study: Annaburroo meteorological data analysis*. 1989. 30 p. + diskette.
- No. 18 Mansbridge, J.V.; Enting, I.G. *Sensitivity studies in a two-dimensional atmospheric transport model*. 1989. 33 p.
- No. 19 O'Brien, D.M.; Mitchell, R.M. *Zones of feasibility for retrieval of surface pressure from observations of absorption in the A band of oxygen*. 1989. 12 p.
- No. 20 Evans, J.L. *Envisaged impacts of enhanced greenhouse warming on tropical cyclones in the Australian region*. 1990. 31 p. [Out of print]
- No. 21 Whetton, P.H.; Pittock, A.B. *Australian region intercomparison of the results of some general circulation models used in enhanced greenhouse experiments*. 1991. 73 p. [Out of print]
- No. 22 Enting, I.G. *Calculating future atmospheric CO₂ concentrations*. 1991. 32 p.
Also electronic edition (718 kB pdf),
at http://www.dar.csiro.au/publications/Enting_2000d.pdf
- No. 23 Kowalczyk, E.A.; Garratt, J.R.; Krummel, P.B. *A soil-canopy scheme for use in a numerical model of the atmosphere — 1D stand-alone model*. 1992. 56 p.
- No. 24 Physick, W.L.; Noonan, J.A.; McGregor, J.L.; Hurley, P.J.; Abbs, D.J.; Manins, P.C. *LADM: A Lagrangian Atmospheric Dispersion Model*. 1994. 137 p.
- No. 25 Enting, I.G. *Constraining the atmospheric carbon budget: a preliminary assessment*. 1992. 28 p. Also electronic edition (571 kB),
at http://www.dar.csiro.au/publications/Enting_2000b.pdf
- No. 26 McGregor, J.L.; Gordon, H.B.; Watterson, I.G.; Dix, M.R.; Rotstayn, L.D. *The CSIRO 9-level atmospheric general circulation model*. 1993. 89 p.
- No. 27 Enting, I.G.; Lassey, K.R. *Projections of future CO₂*. with appendix by R.A. Houghton. 1993. 42 p. Also electronic edition (860 kB pdf),
at http://www.dar.csiro.au/publications/Enting_2000e.pdf
- No. 28 [Not published]
- No. 29 Enting, I.G.; Trudinger, C.M.; Francey, R.J.; Granek, H. *Synthesis inversion of atmospheric CO₂ using the GISS tracer transport model*. 1993. 44 p.
- No. 30 O'Brien, D.M. *Radiation fluxes and cloud amounts predicted by the CSIRO nine level GCM and observed by ERBE and ISCCP*. 1993. 37 p.
- No. 31 Enting, I.G.; Wigley, T.M.L.; Heimann, M. *Future emissions and concentrations of carbon dioxide: key ocean/atmosphere/land analyses*. 1993. 120 p.
- No. 32 Kowalczyk, E.A.; Garratt, J.R.; Krummel, P.B. *Implementation of a soil-canopy scheme into the CSIRO GCM – regional aspects of the model response*. 1994. 59 p.
- No. 33 Prata, A.J. *Validation data for land surface temperature determination from satellites*. 1994. 36 p.
- No. 34 Dilley, A.C.; Elsum, C.C. *Improved AVHRR data navigation using automated land feature recognition to correct a satellite orbital model*. 1994. 22 p.
- No. 35 Hill, R.H.; Long, A.B. *The CSIRO dual-frequency microwave radiometer*. 1995. 16 p.
- No. 36 Rayner, P.J.; Law, R.M. *A comparison of modelled responses to prescribed CO₂ sources*. 1995. 84 p.
- No. 37 Hennessy, K.J. *CSIRO Climate change output*. 1998. 23 p.
- No. 38 Enting, I.G. *Attribution of greenhouse gas emissions, concentrations and radiative forcing*. 1998. 27 p. Also electronic edition (557 kB pdf),
at http://www.dar.csiro.au/publications/Enting_2000c.pdf

- No. 39 O'Brien, D.M.; Tregoning, P. *Geographical distributions of occultations of GPS satellites viewed from a low earth orbiting satellite*. (1998) 28p.
- No. 40 Enting, I.G. *Characterising the temporal variability of the global carbon cycle*. 1999. 53 p. Also electronic edition (636 kB pdf),
at http://www.dar.csiro.au/publications/Enting_2000a.pdf
- No. 41 (in preparation).
- No. 42 Mitchell, R.M. *Calibration status of the NOAA AVHRR solar reflectance channels: CalWatch revision 1*. 1999. 20 p.
- No. 43 Hurley, P.J. *The Air Pollution Model (TAPM) Version 1: technical description and examples*. 1999. 41 p. Also electronic edition (276 kB pdf),
at http://www.dar.csiro.au/publications/Hurley_1999a.pdf
- No. 44 Frederiksen, J.S.; Dix, M.R.; Davies, A.G. *A new eddy diffusion parameterisation for the CSIRO GCM*. 2000. 31 p.
- No. 45 Young, S.A. *Vegetation Lidar Studies*. Electronic edition in preparation.
- No. 46 Prata, A. J. *Global Distribution of Maximum Land Surface Temperature Inferred from Satellites: Implications for the Operation of the Advanced Along Track Scanning Radiometer*. 2000. 30 p. Electronic edition only (8307 kB pdf),
at http://www.dar.csiro.au/publications/Prata_2000a.pdf
- No. 47 Prata, A. J. *Precipitable water retrieval from multi-filter rotating shadowband radiometer measurements*. 2000. 14 p. Electronic edition only (1554 kB pdf),
at http://www.dar.csiro.au/publications/Prata_2000b.pdf
- No. 48 Prata, A.J. and Grant, I.F. *Determination of mass loadings and plume heights of volcanic ash clouds from satellite data*. (in preparation)
- No. 49 (in preparation)
- No. 50 Law, R.M. and Vohralik P.F. *Methane sources from mass-balance inversions: Sensitivity to transport*. Electronic edition only (pdf),
at http://www.dar.csiro.au/publications/Law_2001a.pdf
- No. 51 Meyer, C.P., Galbally, I.E., Wang, Y.-P., Weeks, I.A., Jamie, I. and Griffith, D.W.T. *Two automatic chamber techniques for measuring soil-atmosphere exchanges of trace gases and results of their use in the OASIS field experiment*. Electronic edition only (pdf),
at http://www.dar.csiro.au/publications/Meyer_2001a.pdf

Address and contact details: CSIRO Atmospheric Research
Private Bag No.1 Aspendale Victoria 3195 Australia
Ph: (+61 3) 9239 4400; fax: (+61 3) 9239 4444
e-mail: chief@dar.csiro.au

Last updated 19 April 2001